



Targeting the Genome-Stability Hub Ctf4 by Stapled-Peptide Design

Yuteng Wu, Fabrizio Villa, Joseph Maman, Yu Heng Lau, Lina Dobnikar, Aline C. Simon, Karim Labib, David R. Spring,* and Luca Pellegrini*

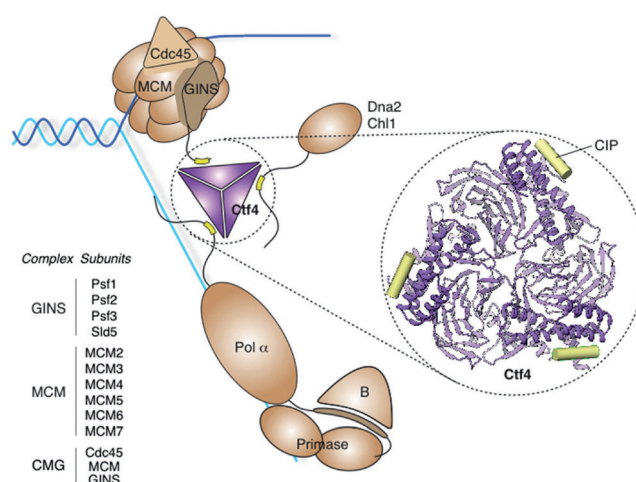
Abstract: The exploitation of synthetic lethality by small-molecule targeting of pathways that maintain genomic stability is an attractive chemotherapeutic approach. The Ctf4/AND-1 protein hub, which links DNA replication, repair, and chromosome segregation, represents a novel target for the synthetic lethality approach. Herein, we report the design, optimization, and validation of double-click stapled peptides encoding the Ctf4-interacting peptide (CIP) of the replicative helicase subunit Sld5. By screening stapling positions in the Sld5 CIP, we identified an unorthodox *i,i+6* stapled peptide with improved, submicromolar binding to Ctf4. The mode of interaction with Ctf4 was confirmed by a crystal structure of the stapled Sld5 peptide bound to Ctf4. The stapled Sld5 peptide was able to displace the Ctf4 partner DNA polymerase α from the replisome in yeast extracts. Our study provides proof-of-principle evidence for the development of small-molecule inhibitors of the human CTF4 orthologue AND-1.

Targeting cancer cells with DNA-damaging agents such as cisplatin is a mainstay of traditional chemotherapy, and its effectiveness might reflect the underlying fragility of cancer cells in maintaining their genomic stability.^[1] More recently, the concept of synthetic lethality as the Achilles heel of cancer cells with defective pathways of genome stability maintenance has taken firm hold since the pioneering observations that breast cancer susceptibility protein 2 (BRCA2)-null cancer cells are exquisitely sensitive to inhibitors of poly(ADP-ribose) polymerase (PARP).^[2,3] Alongside DNA-damaging agents, small-molecule inhibitors of proteins with essential roles in DNA synthesis, such as the DNA polymerase inhibitor fludarabine^[4,5] and the topoisomerase inhibitors camptothecin and etoposide,^[6,7] are currently used in clinical practice. As DNA replication and repair processes

cooperate to preserve genomic integrity, synthetic lethality effects might exist, and should be searched for, among all chromosome instability (CIN) genes.

A distinctive feature of metabolic processes such as DNA replication, repair, and transcription is the high degree of conservation of their protein components among eukaryotes. This observation has recently been exploited to screen CIN genes in yeast, as a quick way of identifying potentially druggable candidates displaying synthetic lethality with DNA repair genes that are often mutated in human cancers.^[8,9] Such an analysis highlighted Ctf4 (chromosome transmission fidelity 4)^[10,11] as a highly promising candidate, at the center of a web of negative genetic interactions with other CIN genes. Moreover, the same appears to be true for the human orthologue of yeast Ctf4, AND-1.^[12] The high level of genetic connections involving Ctf4 is likely to reflect its known role as a protein hub, linking different processes pertaining to chromosome stability, such as DNA replication and sister chromatid cohesion^[13,14] (Scheme 1).

Ctf4 does not possess intrinsic enzymatic activity and therefore lacks an active site, making it harder to target with traditional small-molecule screening strategies. Our recent work has elucidated a key mechanism of recruitment to Ctf4 of its protein partners. Binding is mediated by a short linear



Scheme 1. The drawing summarizes our current understanding of Ctf4 function in the eukaryotic replisome, as a protein hub connecting replisome components such as the DNA helicase CMG (Cdc45–MCM–GINS) and DNA polymerase α , as well as other factors such as the Dna2 helicase–nuclease and the Chl1 helicase. The oval inset shows a ribbon representation of the Ctf4_{CTD} trimer in purple, with bound CIPs as yellow cylinders. Note that the CMG helicase comprises Cdc45, the GINS heterotetramer (made up of the Psf1, Psf2, Psf3, and Sld5 subunits) and the MCM2-7 heterohexamers. The CIP of the CMG helicase is located within the Sld5 subunit of GINS.

[*] Dr. Y. Wu, Dr. Y. H. Lau, L. Dobnikar, Prof. D. R. Spring
Department of Chemistry, University of Cambridge
Cambridge CB2 1EW (UK)

E-mail: spring@ch.cam.ac.uk

Dr. F. Villa, Prof. K. Labib

MRC protein phosphorylation and ubiquitylation unit
University of Dundee
Dundee DD1 5EH (UK)

Dr. J. D. Maman, Dr. A. C. Simon, Prof. L. Pellegrini
Department of Biochemistry, University of Cambridge
Cambridge CB2 1GA (UK)

E-mail: lp212@cam.ac.uk

Dr. Y. H. Lau

Current address: School of Chemistry
The University of Sydney (Australia)

Supporting information and the ORCID identification number(s) for the author(s) of this article can be found under:

<https://doi.org/10.1002/anie.201705611>.

motif (SLIM),^[15,16] known as the Ctf4 interacting peptide (CIP), which docks in α -helical form onto an exposed site on the helical domain of Ctf4, fused to the second β -propeller domain of Ctf4 (Figure 1).^[13,14] The interaction is of moderate, micromolar affinity and represents an example of the SLIM–protein interactions that characterize the dynamic architec-

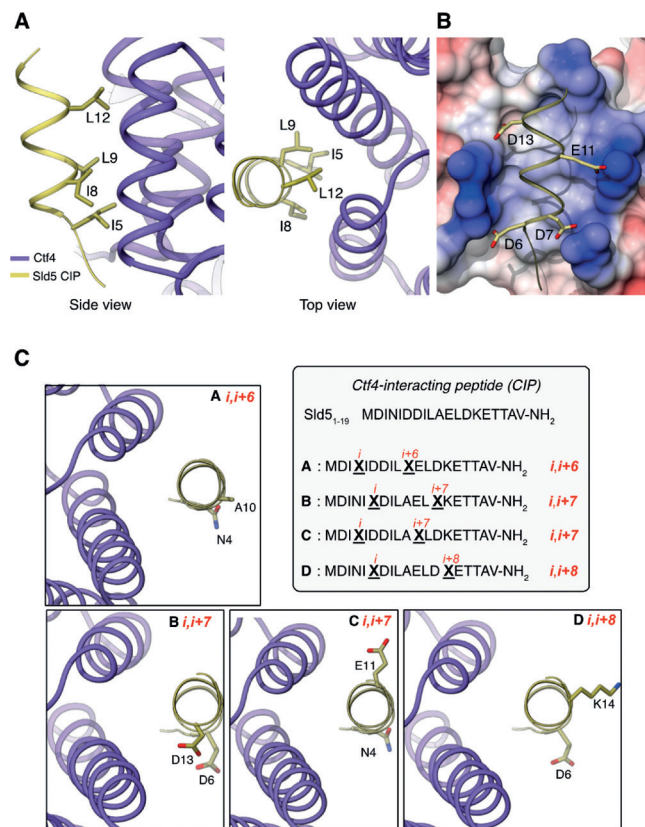


Figure 1. A) Two views of the Ctf4_{CTD}–Sld5 CIP interface (PDB No. 4c95). B) Front view of the Ctf4_{CTD}–Sld5 interface. Ctf4 is shown as a molecular surface, colored according to electrostatic potential, from blue (10 kcal mol⁻¹ e⁻¹) to red (–10 kcal mol⁻¹ e⁻¹). The Sld5 CIP is shown as a ribbon, with the side chains of acidic residues drawn as sticks. C) Sequence of the wild-type Sld5 CIP and of the A, B, C, and D peptides. The stapling positions in each peptide are marked as X (all X = Orn(N₃)). The stapling positions of the A, B, C, and D peptides are also shown mapped onto the structure of the Sld5 CIP bound to Ctf4_{CTD}, in four separate panels.

ture of the replisome.^[17] The ability of Ctf4 to act as a protein hub depends on its trimerization state, which allows it to interact simultaneously with multiple partners.^[13,14] Previous evidence had shown that the three binding sites in the Ctf4 trimer are independent.^[13,14] At present, there is no clear indication whether binding of client proteins to Ctf4 is regulated. The determination of the structural basis for the interaction of Ctf4 with its client proteins has afforded an opportunity to develop a strategy for targeting Ctf4 by interfering with its function as a protein hub.

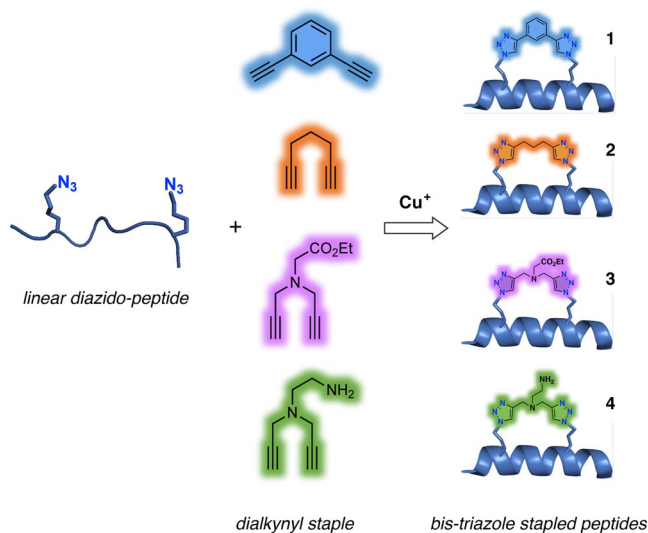
Targeting protein–protein interfaces (PPIs), as a means of specifically disrupting the association between macromolecules, would greatly increase the range of druggable protein

targets, and a lot of effort has gone into developing effective PPI inhibitors.^[18–20] The application of small-molecule approaches to inhibit PPIs can be challenging as such interfaces usually consist of large and relatively flat surfaces, although some notable successes have been reported.^[21,22] A promising approach to generate α -helical PPI inhibitors is the use of conformationally constrained peptides, often referred to as “stapled peptides”, especially when referring to a peptide constrained into an α -helical conformation.^[23–25] In addition to their potential value as inhibitors, stapled peptides represent useful proof-of-principle tools to identify targetable interactions of interesting proteins with their physiological partners and to dissect biological pathways.

Peptide stapling is a macrocyclization approach in which helical peptides are covalently modified through the formation of a chemical linkage (staple) between the side chains of two amino acids.^[26] The residues to be linked together are usually located on the same face of the peptide helix and separated by one, two, or three helical turns, so that one amino acid at position *i* is linked to position *i* + 4, *i* + 7, or *i* + 11, respectively. Stapling can constrain α -helical peptides into their bioactive conformation, improving target affinity and overall pharmacokinetics.^[27] Complementary stapling approaches using doubly cysteine-modified peptides have also been developed.^[28]

When optimized, peptide stapling can generate potent inhibitors of intracellular PPI targets.^[29–33] We have recently pioneered a two-component double-click stapling technique that makes use of a double Cu^I-catalyzed azide–alkyne cycloaddition (CuAAC) between diazido peptides with dialkynyl staple linkages.^[34,35] This approach enables a range of different stapled peptides to be efficiently generated by reacting a single linear diazido peptide with a collection of different dialkynyl stapling linkages (Scheme 2).

Herein, we describe the design of a stapled peptide targeting the interaction of Ctf4 with its client proteins, based



Scheme 2. Double-click peptide stapling. The diazido peptide is combined with different dialkynyl staples under Cu^I catalysis to obtain several bis(triazole) stapled peptides.

on the CIP sequence present in the GINS Sld5 subunit of the replicative helicase complex Cdc45–MCM–GINS (CMG).^[13] The most effective stapled peptide bound to Ctf4 in the same fashion as the wild-type sequence, as determined by X-ray crystallography of the Sld5 CIP bound to the Ctf4 C-terminal domain (Ctf4_{CTD}), but with about tenfold increased affinity. Interestingly, the α -helix of the stapled peptide was conformationally constrained by an unorthodox $i,i+6$ spacing; to the best of our knowledge, this is the first time that the $i,i+6$ constraint has been used to improve helical content and target binding. Furthermore, the stapled CIP was able to disrupt the biochemical interaction between Ctf4_{CTD} and GINS in vitro and to detach the Ctf4 client protein DNA polymerase α from the replisome in yeast extracts. Our study provides the first proof-of-principle evidence that it is possible to develop chemical tools to target the Ctf4 hub in the eukaryotic replisome.

We had previously found that the GINS subunit Sld5 helps to anchor Ctf4 to the CMG helicase, and showed that binding is mediated by the interaction of a short sequence motif of Sld5 (Sld5 CIP; 1-MDINIDDILAELDKETTAV-19) with an exposed site in the helical domain of the Ctf4_{CTD} structure^[13] (Figure 1 A). Alanine-scanning mutagenesis had revealed that the hydrophobic amino acids I5, I8, and L9 at the binding interface were critical for interaction with Ctf4, and that L12 contributed to the interaction (Figure 1 A).^[13] In addition to the hydrophobic interactions, the Ctf4–Sld5 interface displays an electrostatic character owing to charge complementarity between the acidic CIP motif and the basic residues lining the CIP-binding site in Ctf4 (Figure 1 B).

Keeping the key residues in place, four different stapling positions were designed into the Sld5 sequence by inspection of the Ctf4_{CTD}–Sld5 complex structure (PDB No. 4c95), including two sequences with conventional stapling at $i,i+7$ and two with unorthodox $i,i+6$ and $i,i+8$ stapling (Figure 1 C). The diazido peptides CF-A, CF-B, CF-C, and CF-D (Figure 1 C), where “CF” represents N-terminal capping with 5(6)-carboxyfluorescein, were synthesized on Rink amide resin by automated solid-phase peptide synthesis. Copper-catalyzed double-click macrocyclizations were subsequently performed with 1,3-diethynylbenzene (staple **1** in Scheme 2) to generate the corresponding bis(triazole) stapled peptides CF-A1, CF-B1, CF-C1, and CF-D1.

The Sld5-based stapled peptides were first evaluated for their ability to bind Ctf4_{CTD} in a fluorescence anisotropy (FP) assay, using peptides that had been N-terminally labeled with carboxyfluorescein. The $i,i+6$ stapled peptide A1 displayed a stronger binding affinity for Ctf4_{CTD} ($K_d = 0.84 \pm 0.19 \mu\text{M}$) than the wild-type peptide Sld5₁₋₁₉ ($K_d = 3.5 \pm 0.2 \mu\text{M}$) whereas the $i,i+7$ stapled peptides B1 and C1 ($K_d = 18 \pm 1$ and $6.4 \pm 0.6 \mu\text{M}$, respectively) and the $i,i+8$ peptide D1 ($K_d = 15 \pm 1 \mu\text{M}$) showed weaker binding to Ctf4 (Figure 2 A).

As the Sld5 peptide A1, stapled at positions $i,i+6$, showed the strongest binding to Ctf4_{CTD}, it was further investigated using our double-click stapling strategy to explore different staple scaffolds. The stapled peptide A2, which bears a linear aliphatic staple linkage (staple **2** in Scheme 2), was able to bind to Ctf4_{CTD} with a K_d value of $0.32 \pm 0.02 \mu\text{M}$ (Figure 2 B; see also the Supporting Information, Figure S1). Alternative

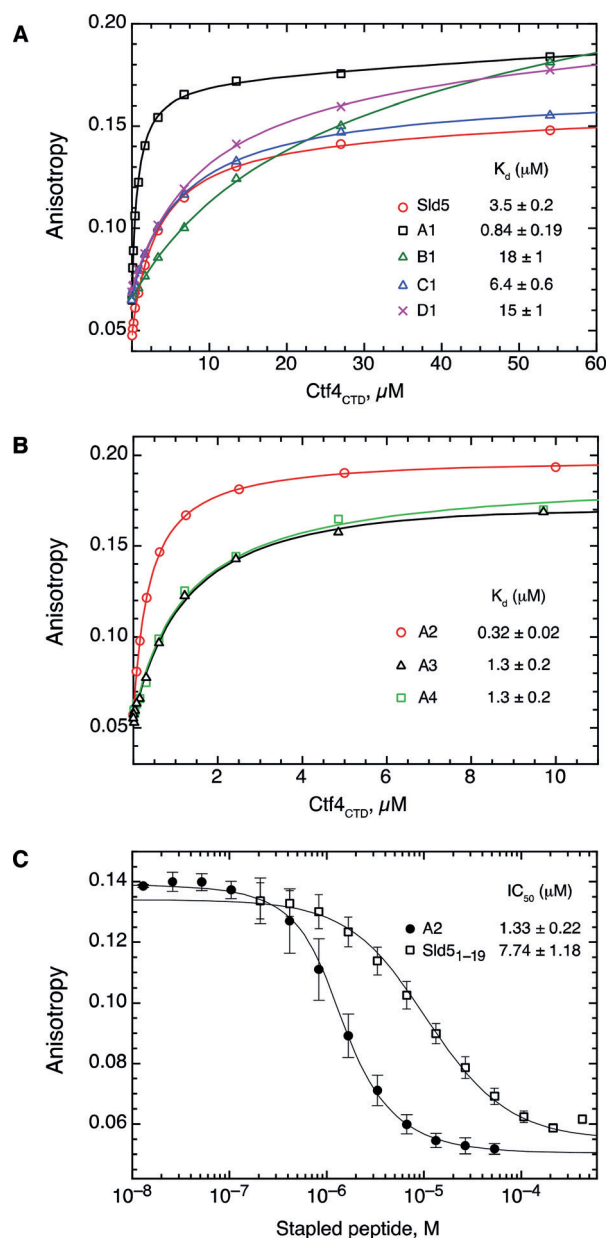


Figure 2. A) Fluorescence polarization (FP) measurements of the affinity of stapled Sld5 CIPs towards Ctf4_{CTD}. Concentration values in A and B refer to the Ctf4_{CTD} protomer. A) FP curves for stapled peptides A1 to D1, which differ in stapling position. The binding curve for the unstapled Sld5 CIP (Sld5 amino acids 1 to 19) is also reported. B) FP curves for Sld5 CIPs stapled at $i,i+6$ (position A) with staple scaffolds 2 to 4. C) FP competition experiment between wild-type Sld5 CIP and the stapled A2 peptide.

aliphatic staples **3** and **4** (Scheme 2) were also investigated; the corresponding stapled peptides A3 and A4 bound to Ctf4_{CTD} with comparable K_d values of $1.3 \pm 0.2 \mu\text{M}$, better than the wild-type peptide but not as tightly as A2 (Figure 2 B). However, the linkers in A3 and A4 provide attachment points for chemical derivatization of the staple, which could be exploited for instance to improve cell permeabilization,^[29,31] while still retaining dissociation constants that are 2.7-fold lower than that of the wild-type peptide.

FP analysis of A2 showed that its binding to Ctf4_{CTD} was one order of magnitude stronger than that of the wild-type peptide (Sld5₁₋₁₉). To confirm this improvement in the binding strength to Ctf4, we performed a competition experiment, challenging the bound fluorescently labeled A2 peptide with unlabeled Sld5₁₋₁₉ or A2 peptides (Figure 2C). The experiment showed that the A2 peptide is a better competitor for Ctf4 binding ($IC_{50} = 1.33 \pm 0.22 \mu\text{M}$) than the wild-type Sld5₁₋₁₉ peptide ($IC_{50} = 7.74 \pm 1.18 \mu\text{M}$).

In the crystal structure of Ctf4_{CTD} bound to the Sld5 CIP, the peptide adopts a two-turn α -helical fold^[13] (Figure 1A). We set out to investigate whether the Sld5 CIP is intrinsically unfolded in solution, and whether stapling might promote the α -helical structure in the A2 peptide, which could explain its higher affinity for Ctf4. Circular dichroism (CD) analysis of Sld5₁₋₁₉ and A2 peptides indicated that they are largely unfolded in aqueous buffer, and that addition of trifluoroethanol (TFE) induced partial α -helix formation in both peptides, as expected (Figure S2).

In the absence of TFE, however, we noticed a 14% difference in α -helical content between the two peptides; whereas the wild-type Sld5 peptide is only 7% helical, the α -helix content of A2 is 21%, three times higher than that of the wild type. Conversely, CD analysis of diazido peptide A, the modified peptide prior to double-click chemistry, suggests that its helical content is only 3% (Figure S2). The physical linkage between residues *i* and *i* + 6 in the A2 peptide might be responsible for its higher intrinsic α -helical content, which would account for its stronger binding to Ctf4.

To determine whether the mode of binding of A2 to Ctf4_{CTD} was as originally observed in the Ctf4_{CTD}-Sld5 CIP structure^[13] and to elucidate the conformation of the stapled Sld5 peptide bound to Ctf4_{CTD}, we determined the X-ray crystal structure of the Ctf4_{CTD}-A2 complex by soaking the stapled peptide in crystals of Ctf4_{CTD} (Table S1). The coordinates and structure factors are deposited in the Protein Data Bank under accession code 5NXQ. Interestingly, a reproducible improvement in the diffraction properties of the Ctf4_{CTD} crystals was observed upon soaking of the A2 peptide, which was not observed in the original soaking experiments with the Sld5 CIP, providing further, indirect evidence that A2 has a stronger affinity for Ctf4_{CTD}.

The experiment showed that A2 binds Ctf4_{CTD} in the same way as the wild-type Sld5 CIP^[13] (Figure 3). In the structure, the bis(triazole) linker is located on the opposite side of the A2 peptide relative to the Sld5 CIP-Ctf4_{CTD} interface, thus achieving the conformation that had originally been planned. The linker is fully exposed to solvent and must therefore cause the higher affinity of the A2 peptide by facilitating the adoption of the correct helical conformation for Ctf4_{CTD} binding. The structure further shows that the triazole ring proximal to stapling position *i* packs against the salt link between Sld5 D7 and Ctf4 R904, providing further stabilization of the stapled Sld5 CIP-Ctf4_{CTD} interface. Surprisingly, the presence of the non-orthodox *i,i* + 6 staple caused no significant difference in conformation between the Ctf4-bound A2 and Sld5 peptides (Figure 4).

Our structural analysis offers a possible rationale for the different affinities resulting from the choice of stapling

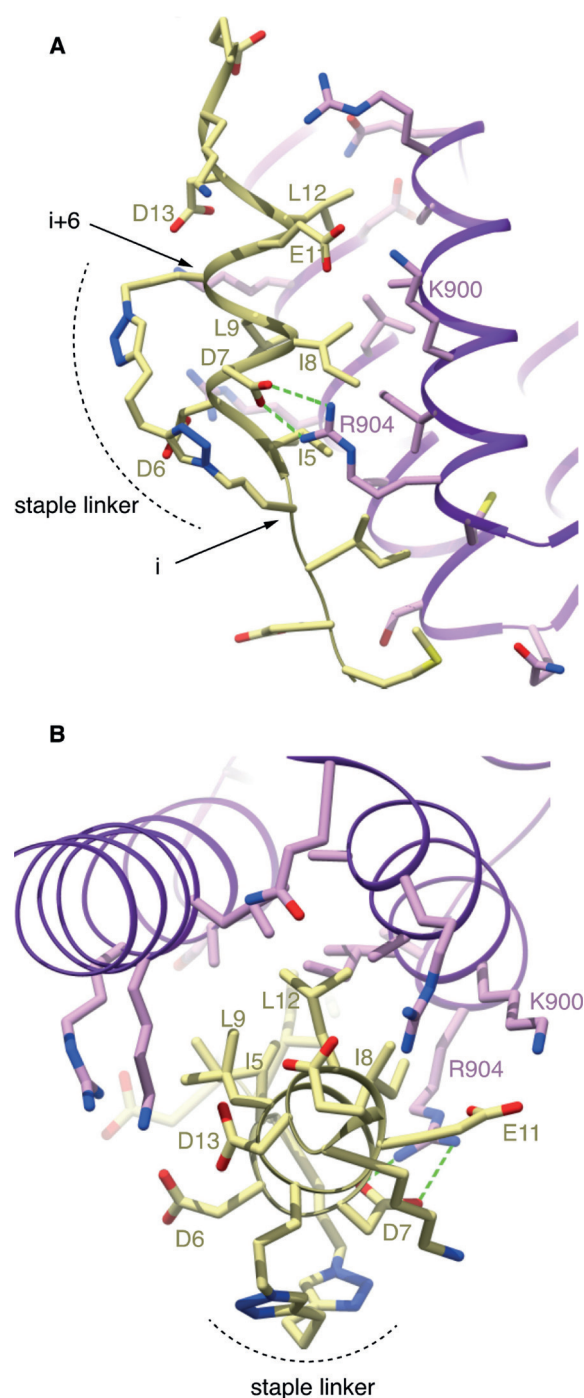


Figure 3. X-ray crystal structure of Ctf4_{CTD} bound to the A2 peptide. A) Side view of the structure drawn as ribbons, in khaki (A2) and purple (Ctf4). The side chains of amino acids discussed in the text are shown as sticks. The stapling positions *i* and *i* + 6 are indicated by arrows. B) Top view of the structure, drawn and colored as in (A).

positions in the CIP sequence. The size of the linker is unlikely to be a major factor in the reduced affinity of peptides B1, C1, and D1, where the interval between stapling positions is larger, because the spacers of staples 1 and 2 were shown to give optimal binding affinity for *i,i* + 7 stapling, compared to longer spacers.^[29,36] Thus the weaker binding of

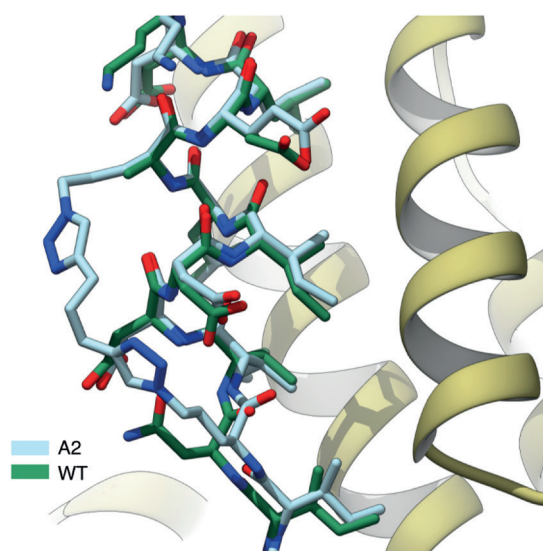


Figure 4. Superposition of the Ctf4_{CTD} structure bound to the stapled A2 peptide and to the wild-type Sld5 CIP (PDB No. 4c95). Ctf4_{CTD} is shown as a light-brown ribbon, and the CIP peptides are drawn as sticks, in cyan (A2) and green (Sld5).

the B1, C1, and D1 peptides relative to A1 might result from the loss of favorable electrostatic interactions provided by D6 and D13 (B1), E11 (C1), or D6 (D1) with the basic residues lining the hydrophobic core of the CIP-binding site in Ctf4 (Figure 1 B, C). In the case of B1, an unfavorable steric effect caused by the position of the staple might also contribute to the loss of affinity.

We next investigated the ability of the wild-type Sld5 CIP and its stapled version A2 to interfere with the interaction between GINS and Ctf4_{CTD}. For this experiment, increasing amounts of peptide were incubated with reconstituted Ctf4_{CTD}-GINS complex, and the samples were analyzed by analytical gel filtration (Figure S3). Addition of both wild-type Sld5 and stapled A2 peptide caused a partial disruption of the Ctf4_{CTD}-GINS complex in a concentration-dependent manner, as demonstrated by the reduction in the peak size for the Ctf4_{CTD}-GINS complex and the increase in the amount of free GINS. The disruptive effect of the Sld5 CIP peptides was noticeable but limited; the incomplete dissociation of the complex is in agreement with previous evidence indicating that the interaction surface between GINS and Ctf4_{CTD} extends beyond the Sld5 CIP binding site.^[13] Nevertheless, at the highest concentration tested in the assay, the stapled peptide A2 was nearly twice as efficient as the wild-type Sld5 CIP (Figure S3).

Our previous work showed that the CIP of Pol1, the catalytic subunit of yeast DNA polymerase α (Pol α), is required for Pol1 to associate with Ctf4 in vitro.^[13] Moreover, mutations in the Pol1 CIP lead to displacement of Pol α from the replisome in yeast cells.^[13] To explore whether it is possible to develop inhibitors of the interaction of Ctf4 with clients such as Pol1, we assayed the ability of the stapled and natural versions of the Sld5 CIP to disrupt the association of Pol α with the replisome in yeast cell extracts. After synchronizing budding yeast cells in S-phase (Figure 5 A),

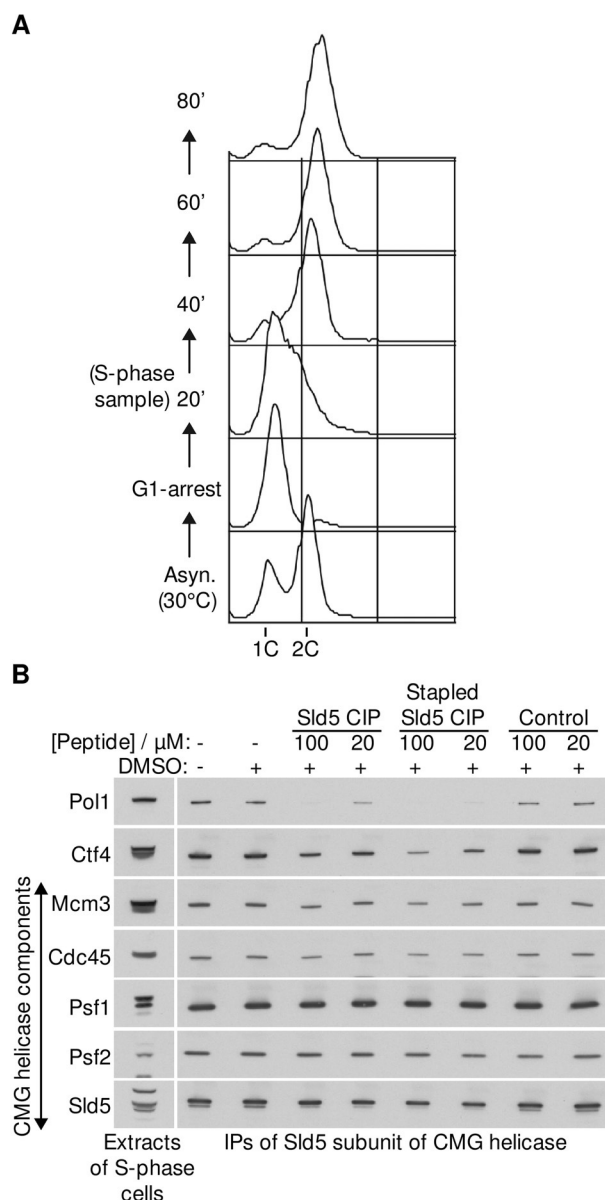


Figure 5. The Sld5 CIP displaces Pol 1 (yeast Pol α) from the replisome in yeast cell extracts. A) *TAP-SLD5* budding yeast cells (YSS47) were grown at 30°C, arrested in G1-phase with mating pheromone, and then released into S-phase for 20 min. The DNA content was measured by flow cytometry. B) The TAP-tagged Sld5 subunit of the CMG helicase was then isolated from cell extracts by immunoprecipitation in the presence of the indicated stapled peptides or controls (the peptides were all dissolved in DMSO), and the indicated proteins were detected by immunoblotting with the corresponding antibodies. Note that the CMG helicase comprises Cdc45, the GINS heterotetramer (made up of the Psf1, Psf2, Psf3, and Sld5 subunits) and the MCM2-7 heterohexamers.

cell extracts were generated and incubated with or without Sld5 CIP or control peptides, before isolation of the replisome by immunoprecipitation of a tagged version of the Sld5 subunit of the CMG helicase (Figure 5 B).

Whereas none of the peptides disrupted the CMG helicase or its interactions with partners such as Csm3, the Sld5 CIP peptides specifically displaced Pol α from the replisome.

Notably, the stapled A2 version of the Sld5 CIP was more effective at lower concentrations than the wild-type Sld5 CIP (Figure 5B). In contrast to the complete disruption achieved for the association of Pol α with the replisome, the stapled version of the Sld5 CIP had a more modest effect on the association of Ctf4 with the CMG helicase (Figure 5B). This is consistent with our past data showing that mutation of the Sld5 CIP does not displace Ctf4 from CMG,^[13] presumably reflecting the more extensive nature of the interaction between Ctf4 and CMG. Nevertheless, these data indicate that the stapled Sld5 CIP can efficiently inhibit the association of replisome-bound Ctf4 with client proteins such as Pol α .

Our preliminary evidence indicates that the A2 peptide displayed limited take-up in yeast cells, which prevented us from assessing its ability to interfere with Ctf4 function in vivo. However, the method allows for a simple approach to garner cell permeability by modification of the staple.^[29,31] Future work will be required to fully explore the potential of stapled peptides to inhibit Ctf4 function in cells and tissues, perhaps by systematic derivatization of the stapling group, which is facilitated by our two-component double-click stapling technique. Furthermore, our proof-of-concept work with stapled peptides will serve to inspire the development of small-molecule inhibitors with different pharmacological properties.

The role of Ctf4 as a hub in the replisome, coupling DNA synthesis to diverse molecular processes that pertain to chromosome replication and segregation, is likely to be conserved in diverse eukaryotic species. For example, the human orthologue of Ctf4 (also known as AND-1 or WDHD1) shares sequence conservation, domain structure, oligomerization state, and physiological roles with its yeast orthologue. It is therefore likely that human CTF4 will represent an attractive therapeutic target in the treatment of cancers carrying defects in CIN genes, and our work raises the prospect that it will be possible to design inhibitors of the interaction of human CTF4 with its client proteins.

Future efforts will be devoted to developing appropriate strategies, including the stapled-peptide approach demonstrated here, to target the biochemical function of CTF4 in human cells. As the type of peptide–protein interaction involving Ctf4 and its partner proteins is likely to represent a paradigm for the dynamic functional architecture of the replisome, such an approach might also be applicable to other instances of PPIs between components of the human replisome.

Acknowledgements

This work was funded by the Wellcome Trust (investigator awards 104641/Z/14/Z to L.P. and 102943/Z/13/Z to K.L.) and the MRC (core grant award MC_UU_12016/13 to K.L.). The Spring laboratory acknowledges support from the European Research Council (FP7/2007-2013)/ERC grant agreement 279337/DOS, the EPSRC, the BBSRC, and the Royal Society.

Conflict of interest

The authors declare no conflict of interest.

Keywords: chemical biology · chromosome stability · Ctf4 protein · protein–protein interactions · stapled peptides

How to cite: *Angew. Chem. Int. Ed.* **2017**, *56*, 12866–12872
Angew. Chem. **2017**, *129*, 13046–13052

- [1] K. Cheung-Ong, G. Giaever, C. Nislow, *Chem. Biol.* **2013**, *20*, 648–659.
- [2] C. J. Lord, A. Ashworth, *Nature* **2012**, *481*, 287–294.
- [3] M. J. O'Connor, *Mol. Cell* **2015**, *60*, 547–560.
- [4] W. Plunkett, P. Huang, V. Gandhi, *Semin. Oncol.* **1990**, *17*, 3–17.
- [5] J. Lukenbill, M. Kalaycio, *Leuc. Res.* **2013**, *37*, 986–994.
- [6] Y.-Q. Liu et al., *Med. Res. Rev.* **2015**, *35*, 753–789.
- [7] K. R. Hande, *Eur. J. Cancer* **1998**, *34*, 1514–1521.
- [8] D. M. van Pel, P. C. Stirling, S. W. Minaker, P. Sipahimalani, P. Hieter, *G3: Genes Genomes Genetics* **2013**, *3*, 273–282.
- [9] K. W. Y. Yuen, C. D. Warren, O. Chen, T. Kwok, P. Hieter, F. A. Spencer, *Proc. Natl. Acad. Sci. USA* **2007**, *104*, 3925–3930.
- [10] N. Kouprina, E. Kroll, V. Bannikov, V. Bliskovsky, R. Gizatullin, A. Kirillov, B. Shestopalov, V. Zakharyev, P. Hieter, F. Spencer, *Mol. Cell. Biol.* **1992**, *12*, 5736–5747.
- [11] J. Miles, T. Formosa, *Mol. Cell. Biol.* **1992**, *12*, 5724–5735.
- [12] D. M. van Pel, I. J. Barrett, Y. Shimizu, B. V. Sajesh, B. J. Guppy, T. Pfeifer, K. J. McManus, P. Hieter, *PLoS Genet.* **2013**, *9*, e1003254.
- [13] A. C. Simon et al., *Nature* **2014**, *510*, 293–297.
- [14] F. Villa, A. C. Simon, M. A. Ortiz Bazan, M. L. Kilkenny, D. Wirthensohn, M. Wightman, D. Matak-Vinkovic, L. Pellegrini, K. Labib, *Mol. Cell* **2016**, *63*, 385–396.
- [15] N. E. Davey et al., *Mol. BioSyst.* **2012**, *8*, 268–281.
- [16] P. Tompa, N. E. Davey, T. J. Gibson, M. M. Babu, *Mol. Cell* **2014**, *55*, 161–169.
- [17] L. Pellegrini, A. Costa, *Trends Biochem. Sci.* **2016**, *41*, 859–871.
- [18] A. P. Higuero, H. Jubb, T. L. Blundell, *Curr. Opin. Pharmacol.* **2013**, *13*, 791–796.
- [19] M. R. Arkin, Y. Tang, J. A. Wells, *Chem. Biol.* **2014**, *21*, 1102–1114.
- [20] L. Lاراia, G. McKenzie, D. R. Spring, A. R. Venkitaraman, D. J. Huggins, *Chem. Biol.* **2015**, *22*, 689–703.
- [21] L. T. Vassilev et al., *Science* **2004**, *303*, 844–848.
- [22] D. Fry, K. S. Huang, P. Di Lello, P. Mohr, K. Müller, S. S. So, T. Harada, M. Stahl, B. Vu, H. Mauser, *ChemMedChem* **2013**, *8*, 726–732.
- [23] L. D. Walensky, G. H. Bird, *J. Med. Chem.* **2014**, *57*, 6275–6288.
- [24] R. Rezaei Araghi, A. E. Keating, *Curr. Opin. Struct. Biol.* **2016**, *39*, 27–38.
- [25] G. L. Verdine, G. J. Hilinski, *Methods Enzymol.* **2012**, *503*, 3–33.
- [26] Y. H. Lau, P. de Andrade, Y. Wu, D. R. Spring, *Chem. Soc. Rev.* **2015**, *44*, 91–102.
- [27] G. H. Bird, E. Mazzola, K. Opoku-Nsiah, M. A. Lammert, M. Godes, D. S. Neuberger, L. D. Walensky, *Nat. Chem. Biol.* **2016**, *12*, 845–852.
- [28] P.-Y. Yang et al., *Proc. Natl. Acad. Sci. USA* **2016**, *113*, 4140–4145.
- [29] Y. H. Lau et al., *Chem. Sci.* **2014**, *5*, 1804–1809.
- [30] Y. H. Lau et al., *Angew. Chem. Int. Ed.* **2015**, *54*, 15410–15413; *Angew. Chem.* **2015**, *127*, 15630–15633.
- [31] W. Xu, Y. H. Lau, G. Fischer, Y. S. Tan, A. Chattopadhyay, M. de la Roche, M. Hyvonen, C. Verma, D. R. Spring, L. S. Itzhaki, *J. Am. Chem. Soc.* **2017**, *139*, 2245–2256.
- [32] Y. S. Chang et al., *Proc. Natl. Acad. Sci. USA* **2013**, *110*, E3445–54.

- [33] A. J. Huhn, R. M. Guerra, E. P. Harvey, G. H. Bird, L. D. Walensky, *Cell Chem. Biol.* **2016**, *23*, 1123–1134.
- [34] Y. H. Lau, Y. Wu, P. de Andrade, W. R. J. D. Galloway, D. R. Spring, *Nat. Protoc.* **2015**, *10*, 585–594.
- [35] M. M. Wiedmann et al., *Angew. Chem. Int. Ed.* **2017**, *56*, 524–529; *Angew. Chem.* **2017**, *129*, 539–544.
- [36] Y. H. Lau, P. de Andrade, G. J. McKenzie, A. R. Venkitaraman, D. R. Spring, *ChemBioChem* **2014**, *15*, 2680–2683.

Manuscript received: June 1, 2017

Revised manuscript received: July 26, 2017

Accepted manuscript online: August 17, 2017

Version of record online: September 7, 2017